SI APPENDIX

Impaired lipid metabolism by age-dependent DNA methylation alterations accelerates aging

Xin Li[1†], JiaQiang Wang[2†], Le Yun Wang[2†], Gui Hai Feng[2†], Gen Li[3†], Meixin Yu[3], Yu Fei Li[2], Chao Liu[2], Xue wei Yuan[2], Guangxi Zang[4], Zhihuan Li[4], Ling Zhao[5], Hong Ouyang[5], Qingli Quan[3], Guangyu Wang[6], Charlotte Zhang[4], Oulan Li[4], Junkai Xiang[8], Jiankang Zhu[7*], Wei Li[2], Qi Zhou[2*] and Kang Zhang[8*]

This PDF file includes:

www.pnas.org/cgi/doi/10.1073/pnas.1919403117

Materials and Methods

Experimental model and subject details

Elovl2 +/- & -/- Mouse

All mouse experiments were performed in accordance with ARRIVE guidelines and regulations. Zygotes were collected from 6-week-old ICR superovulated female mice crossed with ICR males, at post human chorionic gonadotropin (phCG) injection 21h. Cas9 mRNA and sgRNAs targeting Elovl2 exon 3 (Figure S1, 20 ng/μL for each) were injected at phCG 25h. The Cas9 mRNA were in vitro transcribed with mMESSAGEmMACHINE® T7 ULTRA Kit (Ambion, AMB1345-5), and sgRNAs were synthesized by in vitro transcription using MEGAshortscript™ Kit (Ambion, AM1354).

Cell culture and drug treatment

human primary RPE cells were derived from post mortem tissues from an eyebank and were exempted from ethics approval. The human RPE cells were primarily derived from healthy donors. The human fibroblast cells are purchased from ATCC (WI-38, ATCC, CCL-75) Human fibroblasts were maintained in Dulbecco's Modified Eagle Medium (DMEM) supplemented with 10% fetal bovine serum and 50U/ml penicillin-streptomycin. Human RPE cells were cultured with DMEM/F-12 (1:1) supplemented with 10% fetal bovine serum and 50 U/mL penicillin-streptomycin.

For Elovl2 knockdown, lentivector (pLL3.7-shElovl2) exogenously expressing shRNA (5'-TGGTGGTACTATTTCTCCAAA-3') was made and transfected into 293T cells (ATCC) using Lipofectamin 3000 reagent (Thermo Fisher, L3000008) to obtain lentivirus. To build the Elovl2-knockdown cell line, human RPE cells (seeded a night ahead in a concentration of 5×10^5 cells/well) in a 6-well plate were infected with the lentivirus containing Elovl2-shRNA for 24h, followed by 24h of equilibration. Drug treatments were performed at the time of 48h post-

infection. To rescue the Elovl2 knockdown cells, 10 μg/mL curcumin (Sigma, C7727) or 5 mM nicotinamide (Sigma, N0636) or DMSO were added in the cell culture medium and the cells were treated for 48h. H202 treatments were performed on similarly confluent fibroblast cells to avoid variability of H202 effect since H202 toxicity is inversely related to cell density. Briefly, cells on the second day of passage were treated with H202 at the concentration of 100 uM in a single dose for 24 h and then split at a ratio of 1:3 in fresh DMEM with 10%FBS medium followed with SA–β-gal staining.

Method details

RNA extraction, reverse transcription, and qPCR

RNA was extracted by RNeasy Mini Kit (QIAGEN, 74104) and the RNase-Free DNase Set (QIAGEN, 79254) was used to ensure no DNA contamination. Reverse transcription was performed by High Capacity cDNA Reverse Transcription Kit (ABI, 4368814). qPCR was performed by Power SYBR® Green PCR Master Mix (ABI, 4367659). All primers were designed using PrimerPremier5 (Table S1), and synthesized from Integrated DNA Technologies.

Beta-galactosidase staining

SA–β-gal staining was done using a SA–β-gal staining kit (catalog no. 9860; Cell Signaling Technology, Danvers, MA, USA) according to the manufacturer's instructions. Briefly,1.Remove growth media from the cells. 2. Rinse the plate one time with 1X PBS (2 ml or a 35 mm well plate, or match volume of media) 3. Add 1 ml of 1X Fixative Solution to each 35 mm well. Allow cells to fix for 10-15 min at room temperature. 4. Rinse the plate two times with 1X PBS 5. Add 1 ml of the β-Galactosidase Staining Solution to each 35 mm well 6. Incubate the plate at 37°C at least overnight in a dry incubator (no CO2). 7. While the β-galactosidase is still on the plate, check the

cells under a microscope (200X total magnification) for the development of blue color. 8. For long-term storage of the plates, remove the β-Galactosidase staining solution and overlay the cells with 70% glycerol. Store at 4°C.

Western blot

Fresh tissue suspension was obtained by mechanical trituration. Human fibroblast cells and human RPE cells were collected and lysed in Pierce IP Lysis Buffer (Pierce, 87787), supplied with Protease Inhibitor Cocktail (Pierce, 78441) and sodium orthovanadate (Sigma, S6508) on ice for 30min. After 13,000g centrifugation for 10min at 4℃, supernatants were collected and mixed with 30 μL sample buffer (10 mL; 1.25 mL 0.5 M-pH 6.8-Tris-HCl, 2.5 mL glycerin, 2 mL 10% SDS, 200 μL 0.5% bromophenol blue, 3.55 mL H2O, and 0.5 mL β-mercaptoethanol) and incubated for 5 minutes in boiling water. The samples were separated on SDS-PAGE with a 5% stacking gel (10 mL; 5.7 mL ddH2O, 2.5 mL 1.5M pH 6.8 Tris-HCl, 1.7 mL 30% acrylamide (acryl:bis acryl = 29:1), 100 μL 10% SDS, 50 μL 10% ammonium persulfate, and 10 μL TEMED) and a 10% separating gel (10 mL; 4.1 mL ddH2O, 2.5 mL 1.5M pH 8.8 Tris-HCl, 3.3 mL 30% acrylamide (acryl:bis acryl = 29:1), 100 μL 10% SDS, 50 μL 10% ammonium persulfate, and 5 μL TEMED) at 100 V for 1h, and then electrophoretically transferred onto a nitrocellulose membrane at 200 mA for 1h at 4°C. Membranes were blocked in TBST buffer (10 mM Tris, 150 mM NaCl, 0.1% Tween 20, pH 7.4) containing 3% BSA (Sigma, B2064), for 1h at RT and then incubated with primary antibody, diluted in TBST containing 1% BSA, overnight at 4°C. After three washes for 10 minutes each in TBST, the membrane was incubated for 1h at RT with the secondary antibody diluted in TBST. After three washes for 10 minutes each, the signals were detected using ECL and films.

Co-immunoprecipitation

Co-immunoprecipitation of chromatin bound proteins was performed on human fibroblast cells and human RPE cells with the Nuclear Complex Co-IP kit (Active Motif, 54001) following instructions of manufacturer. Briefly, cells were lysed in hypotonic buffer and the nuclear extracts (tight chromatin) were gained via centrifugation. Extracts were digested with enzymatic shearing cocktails and incubate overnight with anti-CHD4 antibody (Sigma, SAB4200107) at 4°C following by the pull-down with protein A/G magnetic beads (Thermo, 88802). The pull-down products were washed, denatured and eluted according to the manufacturer's instruction.

Micro-Computed Tomography Bone Density Analysis

Micro-CT was performed using the Inveon MM system (Siemens, Munich, Germany). Images with 8.82 μm pixel size were acquired under 60 kV of voltage, 300 μA of current and 1,500 ms of exposure time during the 360° rotational step. 2000 slices of images with voxel size of 8.82 μm × 8.82 μm × 8.82 μm were acquired. 3D reconstruction was performed using multimodal 3D visualization software (Inveon Research Workplace, SIEMENS, Munich, Germany).

Open field test

The apparatus consisted of a square-shaped arena (600 × 600 mm^2, length × width) constructed by blue plastic, and illuminated evenly at 15 lux[50]. Test mice were placed facing the center of one wall and allowed to explore the apparatus for 10 min. The open field was subdivided into two virtual concentric squares (center region and all region). The distance and the velocity spent in all regions were calculated.

Morris water maze

The water maze was built with a black tank (2 m diameter) fill with water at room temperature. During the training period, mice were trained to find a fixed platform submerged at constant positions 15 cm below the water surface in one of the quadrant. The mice were placed at four

settled spots in the tank and allowed to find a foothold. If a mouse failed to reach the hidden platform in 90s, it was led to it manually and stayed for 15s. The training of mice was given for 5 days with 2 consecutive trials per day. The natant trajectory was recorded and analyzed with *SMART* image system to calculate the path length, swim velocity and number of turns that mice made. For the spatial learning evaluation, difference between the path length of day1 and day5 was compared. For the spatial memory ability test, the platform was removed from the tank and the mice were released and freely swim in the maze for 90s. The path length, swim velocity and turn numbers were measured.

Accelerating rotarod test

The test was performed with Ugo Basile system following instruction of manufacturer. Briefly, mice were placed on a rotating rod that rotated from 4 to 40 r.p.m. for 5min. The time until falling off or losing balance was recorded. For three consecutive days, each mouse was tested for three trials per day with 30min interval between trials.

Grip strength test

The grip strength test was performed on mice using the TreadScan grip strength measuring system. The mice were allowed to grasp a sensing bar attached to a force strength meter. After reaching the bar with both paws symmetrically, the mice were gently pulled away until the grasp broke. The mean value in five consecutive trails was taken as the score. Results were normalized with body weight (g).

Ultrasonic detection of fatty liver

Ultrasonic scans were acquired with an HDI 5000 scanner (Philips Medical Systems, Bothell, WA), using a broad-bandwidth phased array transducer (2 to 5 MHz). The US images were acquired before biopsy needle insertion; the precise biopsy site was selected based on these

images. Images were acquired with the same presetting of the echographic equipment, i.e., imaging probe, gain, focus and depth range. To avoid operator influence, the US images were recorded without any operator intervention and the TGC was left set by the equipment. Three modes of images based on the frequency band were taken: “Resolution”, high frequency; “Penetration”, low frequency and “Compound”, broad-bandwidth. The images used for defining the biopsy site were stored on a computerized archiving system (PACS) and exported in a DICOM format to a PC (Pentium IV) for further processing. Image analysis was done using a special software package written by the authors in the Matalb® programming environment. Among the three sets of images stored, the images obtained with the lower frequencies, i.e., “Penetration” imaging mode, were the most informative, probably due to the deeper penetration, that allowed useful measurements as far as the diaphragm. Thus, only the “Penetration” images were chosen for further analysis.

Histopathological analysis and oil red O staining

Upon being harvested from animals, murine tissues were fixed in 4% paraformaldehyde (PFA), embedded in paraffin and sectioned. HE staining were performed following standard procedures. Pathological parameters, including necrosis, infiltration of lymphocytes and monocytes, vascular formulation and fibrosis were evaluated.

For the oil red O (ORO) staining, liver tissues were fixed in 4% PFA and equilibrated with 30% sucrose, following with optimal cutting temperature (OCT) compound embedding, snap-freezing and sectioning. ORO staining was performed on cryosections using Lipid (Oil Red O) Staining Kit (Sigma, MAK194). The adipocyte size and numbers were measured using ImageScope-v12.0.1 software.

Lipidomic analysis

For the purpose of lipidomic analysis, liver and brain of mice were harvested and immediately stored in liquid nitrogen until extraction. Plasma were acquired from freshly collected blood by centrifugation and immediately frozen. Lipid extraction was performed following the standard procedure of chloroform-methanol method. The gas chromatography-mass spectrum was performed on the fatty acid extracts with the ?? system according to instructions of the manufacturer. Briefly, a standard curve was built with SPLASH® Lipidomix® Mass Spec Standard (SPLASH, 330707). Levels of saturated fatty acids, monounsaturated fatty acids and poly-unsaturated fatty acids were evaluated.

Glucose tolerance test and Insulin tolerance test

During GTT, an intraperitoneal injection of glucose (Sigma, G7528) with a single dose of 2g/kg body weight was performed in 6h-fasted mice. Blood samples were collected from the tail vein before glucose injection (0 min) and at 15, 30, 60 and 120 min afterward. Blood glucose concentration were immediately measured by a glucose meter (ONETOUCH Ultra, Lifescan).

ITT was performed by intraperitoneal injection of insulin (0.75 IU/Kg, Aladdin, 12584-58-6). Blood glucose concentrations were measured before insulin injection (0 min) and 30, 60, 90 and 120 min after insulin injection. Blood samples were collected from mice tail vain and blood glucose concentration were immediately measured by a glucose meter (ONETOUCH Ultra, Lifescan).

RNA-seq

Liver tissue and human RPE cell samples were collected and send to BGI company to perform RNA-seq.

Total RNA was extracted from cultured cells (1×10^6 cells) by TRIzol reagent (Invitrogen). RNA-Seq sequencing was performed on an Illumina HiSeq 4000 sequencer with 150 bp paired-end sequencing reactions.

The RNA-seq reads of each sample was mapped to the mouse mm9 or human hg19 genome assembly independently by the HISAT2 software (*1*) using the annotated gene structures as templates. Default parameters of HISAT2 were used except with the option "--dta-cufflinks" opening. Reads with unique genome location were reserved for gene expression calculation using Cufflinks (version 2.0.2) with the option "--GTF" (*2*). The heatmaps were produced by the heatmap.2 function of R. Gene ontology analysis of differentially expressed genes were analyzed in DAVID and processes were selected based on p values smaller than 0.05 (*3*). The differentially expressed gene list of mouse liver between aging and young were download from the published data (*4*). And the gene sets comparison between our data and the datasets were performed by Gene Set Enrichment Analysis (GSEA) software (*5*).

Immunofluorescence staining and MitoSOX staining

Murine tissue sample were freshly collected upon perfusion, followed by overnight PFA fixation and sucrose dehydration. Human fibroblast cells, human RPE cells and murine primary cells were fixed with 4% PFA for 1h. To perform immunofluorescence, the slide was rinsed in PBS for 5 minutes, blocked in blocking buffer (PBS with 1% BSA, 0.1% Tween-20) for 20 minutes at room temperature (RT), and incubated with primary antibody in blocking buffer for 1 hour at RT. After 3 washes with 0.1% Tween-20 in PBS, the slide was incubated with secondary antibody in blocking buffer for 1 hour at RT. The slides were mounted with DAPI-Vectashield solution (Vector laboratories). Images were taken with a confocal microscope (LSM 780). To

estimate the mitochondrial conditions, human RPE cells and murine primary cells were incubated with either MitoSOX (5uM) according to manufacturer's instructions.

Glycolysis stress test and Mito stress test

The glycolysis stress test and the mito stress test were performed on murine primary hepatocytes with Seahorse Bioscience XF Analyzer (Agilent Tech) following the instructions of manufacturer. Briefly, the murine hepatocytes were seed in the XF96 cell culture microplate (Seahorse Bioscience, 101085-004) with 100,000 cells per well. Ahead of the assays, the culture medium was replaced followed by 1h incubation in 37℃. For the glycolysis stress test, cell culture medium was replaced by Seahorse XF Base medium (Seahorse Bioscience), supplemented with L-glutamine. During the assay, glucose, oligomycin and 2-deoxyglucose were added into each well sequentially, followed by mixing and measurements. For the mito stress test, culture medium was replaced by Seahorse XF Base medium supplemented with glucose, l-glutamine and pyruvate. During the assay, oligomycin, FCCP and rotenone were added into each well sequentially, followed by mixing and measurements. Mixture time, incubation time and the timeline of chemicals addition were determined based according to instructions of manufacturer.

Fundus Autofluorescence Imaging

An established protocol was used to perform fundus autofluorescence imaging. Briefly, Use a confocal scanning laser ophthalmoscope (Spectralis HRA, Heidelberg Engineering, Heidelberg, Germany). Fundus AF images were acquired using a 488 nm excitation wavelength. Before imaging mice were anesthetized, and kept warm using a temperature control heater. The pupils were dilated with phenylephrine hydrochloride (Mydfrin 2.5%; Alcon) and tropicamide (Mydriacyl 0.5%; Alcon). A drop of Gen Teal Liquid Gel (Novartis, East Hanover, NJ) was

applied to the surface of the cornea to maintain hydration and clarity, and to prevent cataract formation. Adjust the platform to allow appropriate positioning. All images were acquired in the high-speed mode with a 55° field, digitized in frames of 768 × 768 pixels with a resolution of approximately 11 mm per pixel (8.9 frames/second). Imaging started centrally, and extended into the mid and far periphery focusing on the temporal detached quadrant of the retina.

ERG and VEP recording methodology

Unless otherwise stated, recording procedures for the ERG and VEP were identical. The pentobarbital sodium powder was dissolved in normal saline, with a concentration of 1%, Sumianxin with 100% concentration was diluted with saline to 10%. The mice were anesthetized by intraperitoneal injection (and the Sumianxin and pentobarbital sodium should be injected separately). In adult mice, 0.3ml pentobarbital was injected per 100g mice weight, and each mouse was injected with 0.02ml Sumianxin. Body temperature was maintained at 38℃ with a heating pad. Pupils were dilated with Atropine (1%).

The mouse should be dark-adapted for 12 hours in advance, and the mouse that have not been experimented needed to be placed in the dark adaptable box to avoid the flash in the experiment affects the dark environment. For ERG recordings, a gold-wire electrode was placed on the corneal surface of the right eye and referenced to a gold wire in the mandible. A needle electrode in the right forelimb served as the ground. The active electrode for the flash VEP (a steel needle) was placed 3 mm lateral to lambda over the left cortex (contralateral to the stimulated right eye).This location overlies the area of the striate cortex represented by the binocular visual field. The reference electrode was a needle electrode placed in the mandible. The left eye (not stimulated) was occluded with a dark patch for both the ERG and VEP recordings.

For the FERG and FVEP, stimulus production and data collection were carried out with the Visual Electophysiology Instrument (OPTO-III, optoprobe, canada) . The signal was amplified 10,000 band pass filtered (0.5–100 Hz) and digitized at 300 Hz with 12 bits resolution.

Magnetic resonance image acquisition

Axial, sagttial and coronal structure images of 8-week-old adult mice brain were acquired on a 7 Tesla MRI scanner (PharmScan 70/16 US, Bruker, Switzerland). The contrast required for registration and assessment of volume is not acceptable with our typical T2-weighted imaging sequence. Therefore, diffusion-weighted imaging was performed to enhance the contrast between white and grey matter to aid in the registration and volume measurements.

Quantification and statistical analysis

Statistical analyses were performed in R. Levels of significance were calculated with two tailed student's t-test. In all figures: $*$, p-value < 0.05; $**$, p-value < 0.01.

Data Resources

The sequencing data have been deposited in Genome Sequence Archive of Beijing Institute of Genomics, Chinese Academy of Sciences (http://gsa.big.ac.cn/). The accession number for mouse and human data reported in this project are CRA002140 and CRA002141.

Fig. S1

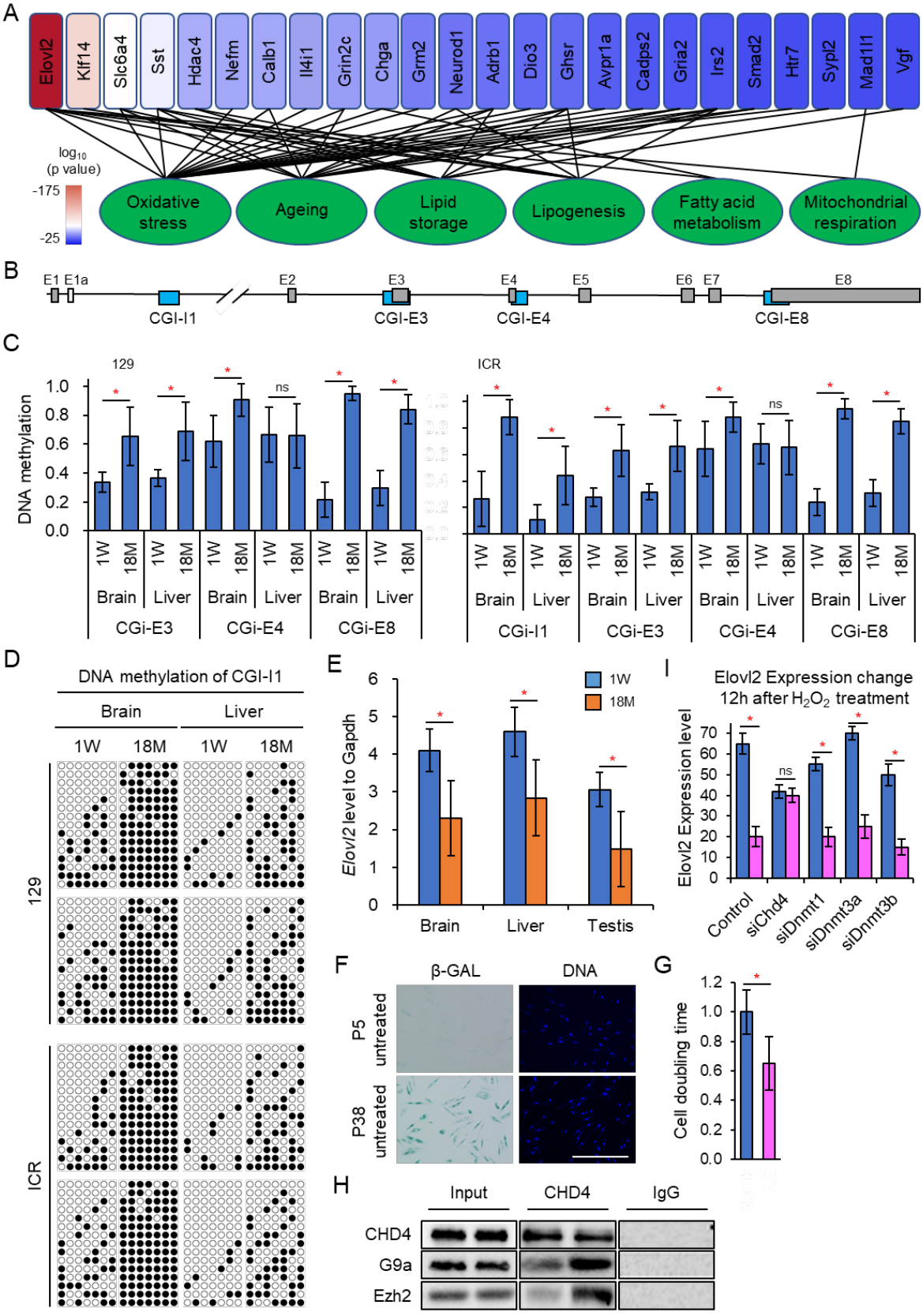
A
Elovl2
Klf14
Slc6a4
Sst
Hdac4
Nefm
Calb1
Il4i1
Grin2c
Chga
Grm2
Neurod1
Adrb1
Dio3
Ghsr
Avpr1a
Cadps2
Gria2
Irs2
Smad2
Htr7
Sypl2
Mad1l1
Vgf
log10 (p value)
-175
-25
Oxidative stress
Ageing
Lipid storage
Lipogenesis
Fatty acid metabolism
Mitochondrial respiration
B
E1 E1a
E2
E3
E4
E5
E6 E7
E8
CGI-I1
CGI-E3
CGI-E4
CGI-E8
C
129
ICR
DNA methylation
1W
18M
Brain
Liver
CGi-E3
CGi-E4
CGi-E8
CGi-I1
D
DNA methylation of CGI-I1
Brain
Liver
1W
18M
129
ICR
E
Elovl2 level to Gapdh
1W
18M
Brain
Liver
Testis
I
Elovl2 Expression change
12h after H2O2 treatment
Elovl2 Expression level
Control
siChd4
siDnmt1
siDnmt3a
siDnmt3b
F
β-GAL
DNA
P5 untreated
P38 untreated
G
Cell doubling time
H
Input
CHD4
IgG
CHD4
G9a
Ezh2

Fig. S1 Elovl2 is a metabolic gene that serves as marker of aging. **(A)** Gene function of top Epigenetic aging markers. (B)The structure of Elovl2 in mouse. **(C)** The DNA methylation levels on the CpG islands of intron 1 (I1) and exon 3, 4, and 8 (E3, 4, 8) of Elovl2 in brain and liver of 129/sv and ICR mice. Error bars, standard error of the mean (SEM). *, $p < 0.05$. Levels of significance were calculated with two tailed student's t-test. **(D)** The DNA methylation level on CGi-I1 in brain and liver of mice at the age of 18 months was significantly higher than that of 1 week. **(E)** *Elovl2* expression level decrease along with age. *, $p < 0.05$. Levels of significance were calculated with two tailed student's t-test. **(F)** Beta-galactosidase (β-GAL) staining on young (p5) and old (p38) human fibroblast cells. Scale bar = 100 μm. **(G)** Representative statistical chart of cell proliferation (cell number doubling time) of human fibroblast cells with or without hydrogen peroxide (H_2O_2) treatment. *, $p < 0.05$. Levels of significance were calculated with two tailed student's t-test. **(H)** Co-immunoprecipitation results of human fibroblast cells with or without H_2O_2 treatment. Antibody of CHD4, G9a and Ezh2 were used. It showed CDH4 can recruit G9a and Ezh2. **(I)** *Elovl2* expression level significantly decreased after H_2O_2 treatment in groups where DNMT1, DNMT3A or DNMT3B but not CHD4 were knockdown. *, $p < 0.05$. Levels of significance were calculated with two tailed student's t-test.

Fig. S2

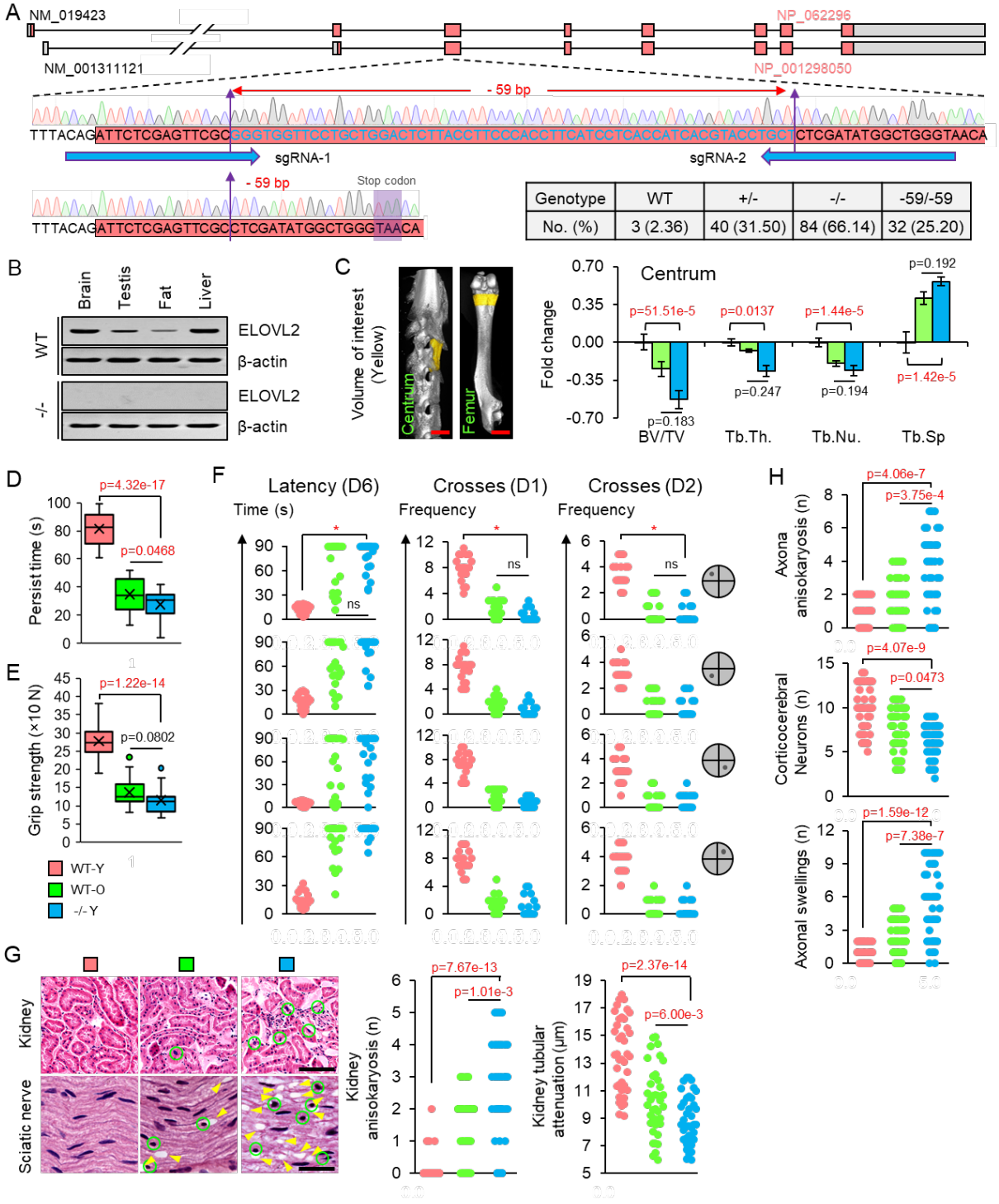

Fig. S2 Deletion of Elovl2 causes dramatic acceleration of aging in mice. (A) The design of sgRNA and genotype of mice in different groups. **(B)** Western blotting showing the expression of

ELOVL2 in different organs of WT or -/- mice. **(C)** Representative images showing the hair loss of WT-O or -/- mice. The bone volume/total volume (BV/TV), trabecular thickness (Tb. Th.), trabecular number (Tb. Nu.) and trabecular spacing (Tb. Sp.) was measured by Micro-CT. Error bars, SEM. Levels of significance were calculated with two tailed student's t-test. Scale bar = 2 mm. **(D & E)** -/- Y mice displayed reductions in endurance (D) and muscle strength (E). Error bars, SEM. Levels of significance were calculated with two tailed student's t-test. **(F)** The Morris Water Maze test showed spatial learning and memory of WT-O and -/- mice were significantly decreased. Error bars, SEM. *, $p < 0.05$. Levels of significance were calculated with two tailed student's t-test. **(G & H)** Representative images of hematoxylin and eosin staining and pathological section analysis of kidney and sciatic nerve; green cycles show the abnormal structures. Scale bar = 100 μm. Levels of significance were calculated with two tailed student's t-test.

Fig. S3

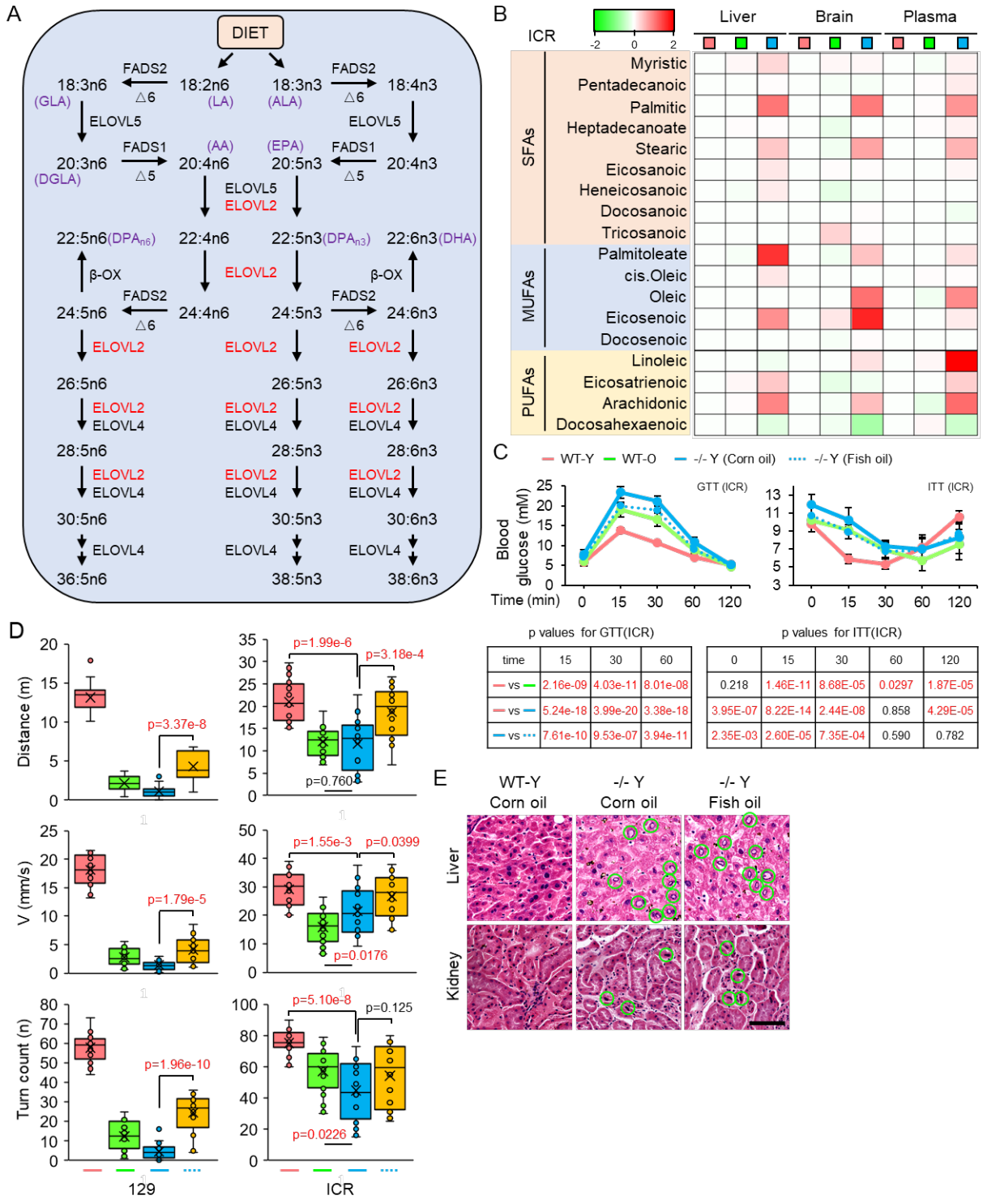

Fig.S3 Multiple metabolic disturbances were found in Elovl2 KO mice. (A) The schematics showing the roles of ELOVL families in lipid metabolism. **(B)** The heat map of fatty acid species,

saturated fatty acids (SFAs), mono-unsaturated fatty acids (MUFAs) and poly-unsaturated fatty acids (PUFAs) in liver, brain and plasma of ICR mice. **(C)** Glucose tolerance test (GTT) (left) and Insulin tolerance test (ITT) (right) for mice on regular diet (Corn oil) and PUFAs adding diet (Fish oil) (n = 12 per group). Error bars, SEM. Levels of significance were calculated with two tailed student's t-test. **(D)** Distance, velocity and turn count of different groups of 129/sv mice and ICR mice fed with either corn oil or fish oil in the open-field test. Levels of significance were calculated with two tailed student's t-test. **(E)** Representative images of hematoxylin and eosin staining and pathological section analysis of liver and kidney from WT-Y, -/- Y fed with corn oil supplemented diet and -/- Y fed with fish oil supplemented diet. Scale bar = 100 μm.

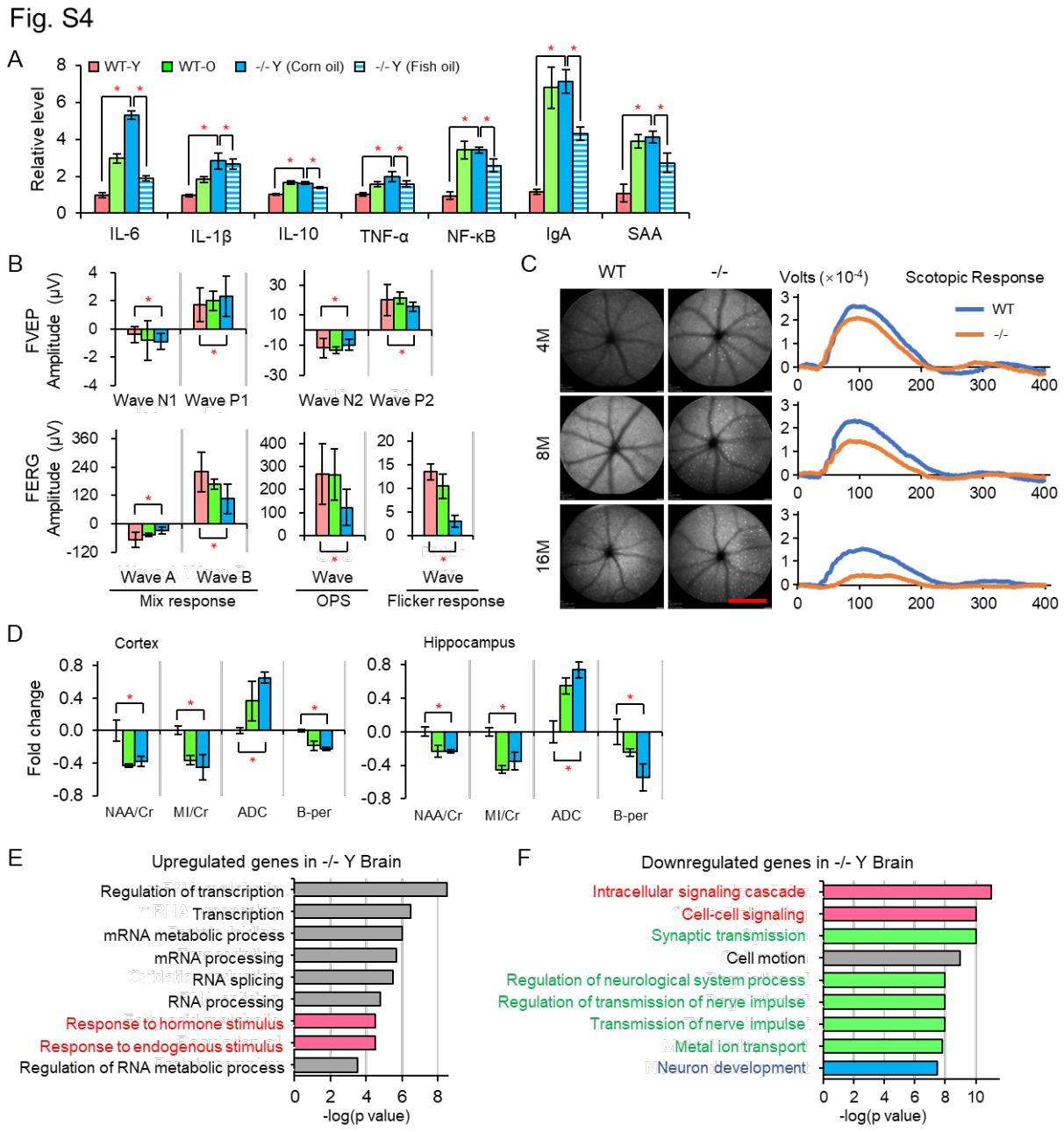

Fig.S4 The depletion of Elovl2 in mice led to chronic inflammation and a decline in the function of eye and brain. (A) ELISA test on inflammatory factors in blood samples from different groups of ICR mice. Error bars, SEM. *, $p < 0.05$. Levels of significance were calculated with two tailed student's t-test. **(B)** ERG and VEP recording methodology analysis showed a decline of eye function. Error bars, SEM. *, $p < 0.05$. Levels of significance were calculated with

two tailed student's t-test. **(C)** Fundus Autofluorescence Imaging showed the appearance of drusen in -/- Y mice. Scale bar = 2 mm. **(D)** magnetic resonance imaging (MRI) analysis on the cerebral cortex and hippocampus. It revealed a dramatic abnormity in -/- Y and WT-O mice. Error bars, SEM. *, $p < 0.05$. Levels of significance were calculated with two tailed student's t-test. **(E & F)** Gene Ontology analysis of the RNA-Seq data revealed disfunction in the brain of -/-Y mice.

Fig. S5

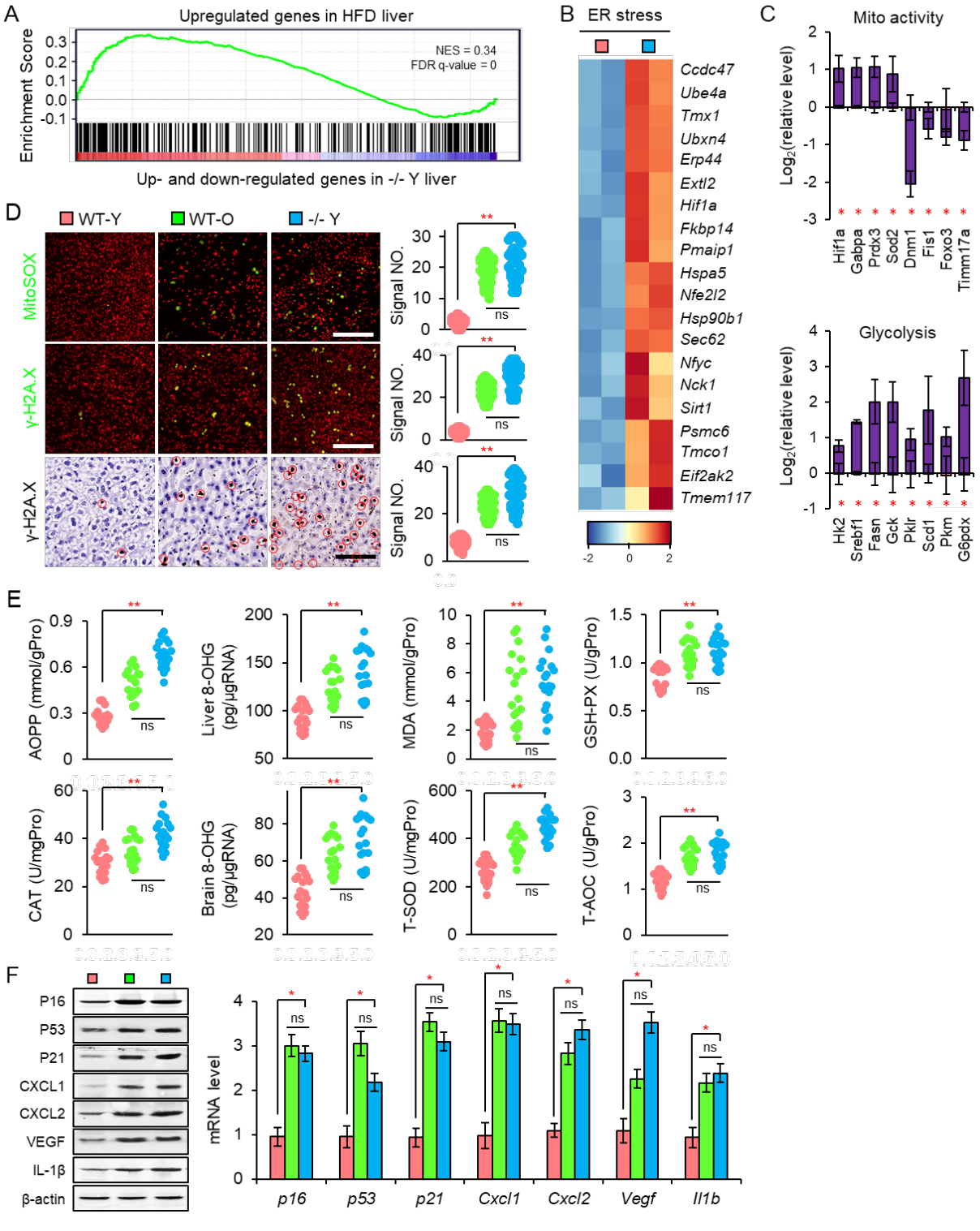
A
Upregulated genes in HFD liver
Enrichment Score
NES = 0.34
FDR q-value = 0
Up- and down-regulated genes in -/- Y liver
B
ER stress
Ccdc47
Ube4a
Tmx1
Ubxn4
Erp44
Extl2
Hif1a
Fkbp14
Pmaip1
Hspa5
Nfe2l2
Hsp90b1
Sec62
Nfyc
Nck1
Sirt1
Psmc6
Tmco1
Eif2ak2
Tmem117
C
Mito activity
Log2(relative level)
Hif1a
Gabpa
Prdx3
Sod2
Dnm1
Fis1
Foxo3
Timm17a
Glycolysis
Hk2
Srebf1
Fasn
Gck
Pklr
Scd1
Pkm
G6pdx
D
WT-Y
WT-O
-/- Y
MitoSOX
γ-H2A.X
γ-H2A.X
Signal NO.
ns
E
AOPP (mmol/gPro)
Liver 8-OHG (pg/μgRNA)
MDA (mmol/gPro)
GSH-PX (U/gPro)
CAT (U/mgPro)
Brain 8-OHG (pg/μgRNA)
T-SOD (U/mgPro)
T-AOC (U/gPro)
F
P16
P53
P21
CXCL1
CXCL2
VEGF
IL-1β
β-actin
mRNA level
p16
p53
p21
Cxcl1
Cxcl2
Vegf
Il1b

Fig. S5 Elovl2 ablation leads to severe oxidative damage at the cellular level. (A) Enriched gene sets of differentially expressed genes in -/- Y samples. The horizontal axis represents the differentially expressed genes in -/- Y compared to high fat diet (HFD) mouse samples which were ranked as either up- or down-regulated in -/- Y and marked in red and blue, respectively. The normalized enrichment score (NES) and false discovery rate (FDR) are marked. **(B)** Expression pattern of genes in ER stress pathways in WT-Y and -/- Y liver samples. **(C)** qPCR results verified the RNA-Seq data. Error bars, SEM. *, $p < 0.05$. Levels of significance were calculated with two tailed student's t-test. **(D)** MitoSOX staining and γH2A.X staining showed sever oxidative damage in mitochondria and nuclei respectively in -/- Y mice. Error bars, SEM. **, $p < 0.01$. Levels of significance were calculated with two tailed student's t-test. Scale bar = 100 μm. **(E)** The oxidative damage affecting proteins (AOPP), lipids (MDA), and RNA (8-OHG). Error bars, SEM. **, $p < 0.01$. Levels of significance were calculated with two tailed student's t-test. **(F)** Higher cellular senescent markers were detected by western blotting and qPCR in -/- Y and WT-O mice. Error bars, SEM. *, $p < 0.05$. Levels of significance were calculated with two tailed student's t-test.

Fig. S6

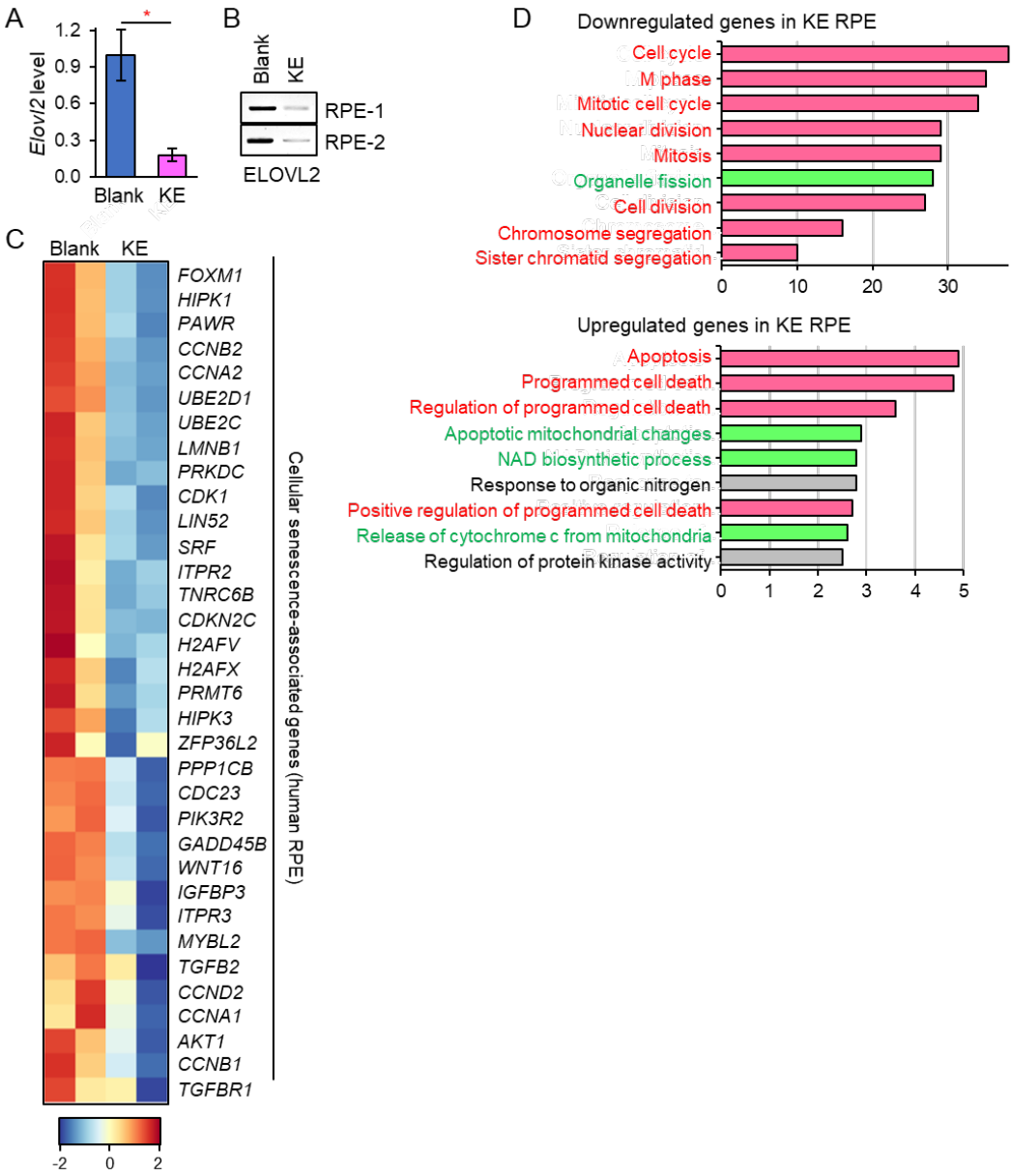

Fig. S6 AMD phenotype was induced by *ELOVL2* deficiency. (A & B) qPCR (A) and Western blotting (B) results showed ELOVL2 expressions in blank and KE human RPE cells. Levels of significance were calculated with two tailed student's t-test. **(C)** Heatmap showing the cluster of cellular senescence-associated genes with variation between blank and KE human RPE cells. **(D)** RNA-seq data revealed the upregulated genes and downregulated genes in KE human RPE cells.

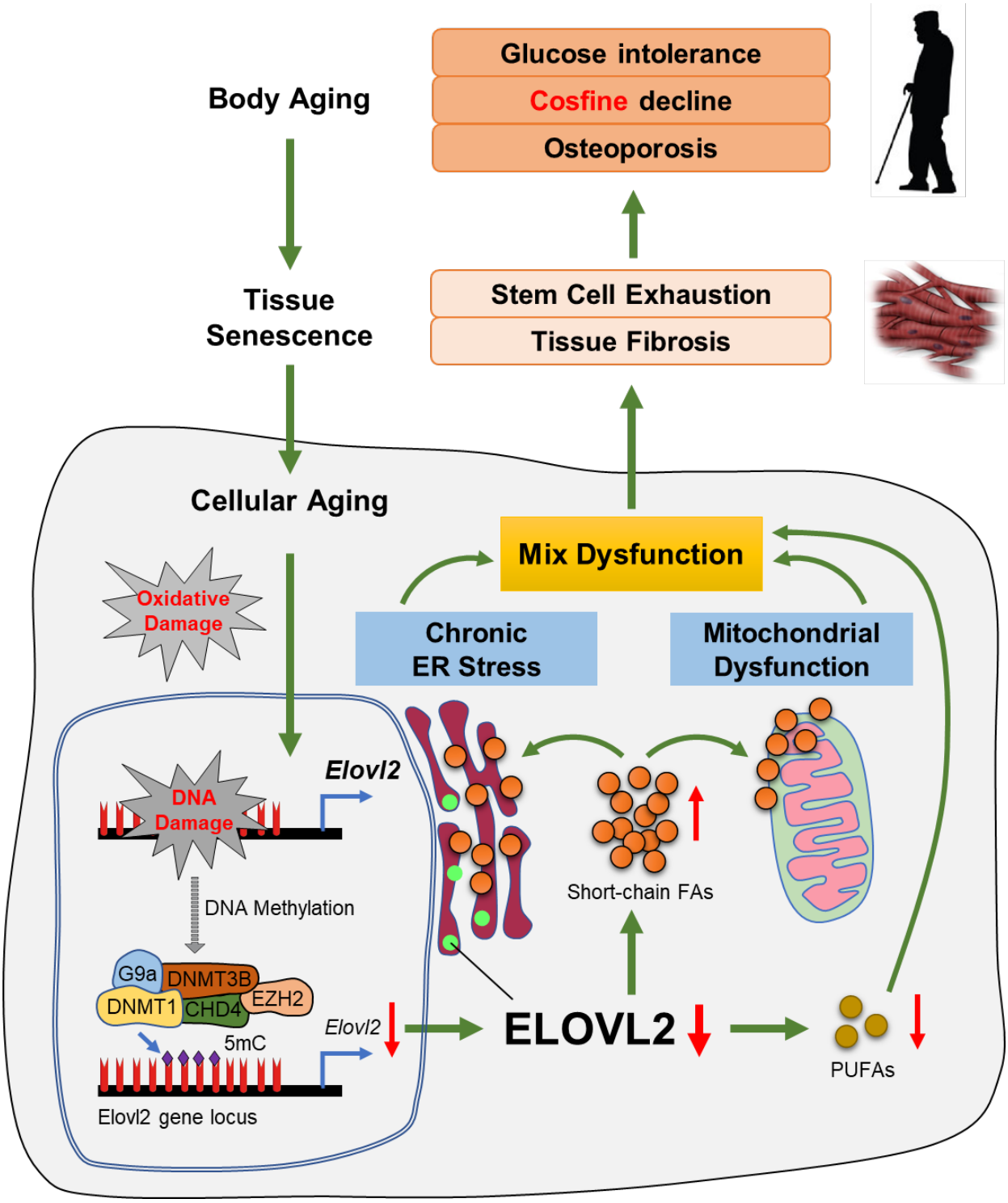

Fig. S7 Schematic of model for age-related DNA methylation mediated accelerated aging process

1. D. Kim, B. Langmead, S. L. Salzberg, HISAT: a fast spliced aligner with low memory requirements. *Nat Methods* **12**, 357-360 (2015).
2. C. Trapnell *et al.*, Transcript assembly and quantification by RNA-Seq reveals unannotated transcripts and isoform switching during cell differentiation. *Nat Biotechnol* **28**, 511-515 (2010).
3. W. Huang da, B. T. Sherman, R. A. Lempicki, Systematic and integrative analysis of large gene lists using DAVID bioinformatics resources. *Nat Protoc* **4**, 44-57 (2009).
4. R. R. White *et al.*, Comprehensive transcriptional landscape of aging mouse liver. *BMC Genomics* **16**, 899 (2015).
5. A. Subramanian *et al.*, Gene set enrichment analysis: a knowledge-based approach for interpreting genome-wide expression profiles. *Proc Natl Acad Sci U S A* **102**, 15545-15550 (2005).